Ion implantation in silicon to facilitate testing of photonic circuits

Graham T. Reed*[a], Milan M. Milosevic[a], Xia Chen[a], Wei Cao[a], Callum G. Littlejohns[a,b], Hong Wang[b], Ali Z. Khokhar[a], David J. Thomson[a]

[a]Optoelectronics Research Centre, University of Southampton, Southampton, UK, SO17 1BJ;

[b]Nanyang Technological University, Singapore, Singapore

ABSTRACT

In recent years, we have presented results on the development of erasable gratings in silicon to facilitate wafer scale testing of photonics circuits via ion implantation of germanium. Similar technology can be employed to develop a range of optical devices that are reported in this paper. Ion implantation into silicon causes radiation damage resulting in a refractive index increase, and can therefore form the basis of multiple optical devices. We demonstrate the principle of a series of devices for wafers scale testing and have also implemented the ion implantation based refractive index change in integrated photonics devices for device trimming.

Keywords: Ion implantation, grating couplers, ring resonators, annealing, trimming.

1. INTRODUCTION

Silicon photonics is at present one of the most buoyant technologies in the world and is particularly regarded as a low cost solution for short reach interconnects for applications in the information and communication sectors, environmental engineering, and healthcare[1-8]. The technology is able to make use of the large silicon manufacturing infrastructure already in existence for microelectronics industry, and is targeting mass markets.

The ring resonator represents one of the basic building block of many photonic circuits. It is widely used for both active and passive devices, and has been used in particular for the development of a number of applications such as lasing, filtering, modulation and sensing, aiming to provide devices that offer compactness and low power consumption. In the last few years it has become more challenging to achieve precise control of positioning and stability of the resonant wavelength peak of micro-ring resonator due to its high sensitivity to fabrication errors and environmental changes. A heater or thermoelectric cooler is typically used to trim the position of the resonant wavelength peak. However, this requires additional power consumption which is one of the key obstacles to development of viable commercial optoelectronic products. Fabrication process and SOI wafer thickness variations induce similar or perhaps even larger resonant wavelength shift than environmental changes thus requiring high power consumption to precisely control the operating wavelength. Therefore, post-fabrication trimming of the ring resonator is investigated by researchers worldwide. For example, electron beam induced compaction and strain[6] to the oxide cladding have been proposed to trim the resonant wavelength peak of silicon ring resonators[7]. However, in this case the refractive index variation of the oxide is quite small, which limits the tuning range. Additionally, it is an expensive and comparatively slow process. Electron beam bleaching of a polymer cladding was also proposed for more effective trimming[8] but it lacks universal CMOS compatibility, and is a similarly slow process.

Ion implantation into silicon causes radiation damage. If a sufficient dose is implanted, complete amorphisation can result in a local part of the device. Amorphous silicon has a refractive index that is significantly different (higher) than that of crystalline silicon ($\sim 10^{-1}$), and can therefore form the basis of multiple optical devices. We have carried out experiments to demonstrate the principle of implementation of a series of devices for wafers scale testing. In addition, we have implemented the ion implantation based refractive index change in a selection of integrated photonic devices, although application to any optical device is possible, particularly resonant structures. Therefore, this reversible refractive index change can be selectively removed to tune the operating wavelength, by selective local annealing. We discuss this approach in the context of both wafer scale testing and active device trimming.

*g.reed@soton.ac.uk; phone +44 23 8059 5494; fax +44 23 8059 5494; www.soton.ac.uk

2. DESIGN AND FABRICATION

Any resonant wavelength shift in a ring resonator depends on the mode effective index and the optical path length at a certain wavelength[3]. The mode effective index at a given temperature depends on the material refractive index, waveguide dimensions, and operating wavelength. We have used Lumerical software[9] for simulation analysis. Standard SOI rib waveguides with 220nm crystalline silicon height (100 nm silicon slab layer) and a 2 µm buried oxide (BOX) layer have been used. For all 500 nm wide silicon waveguides, we have designed and fabricated ring resonators with R=10µm radius, an edge-to edge spacing of Gap=120 nm and different implantation arc length θ = (2°, 6°, 10°, 14°, 18°, 22°) (Figure 1). Un-implanted ring resonators with the same dimensions were also fabricated for reference.

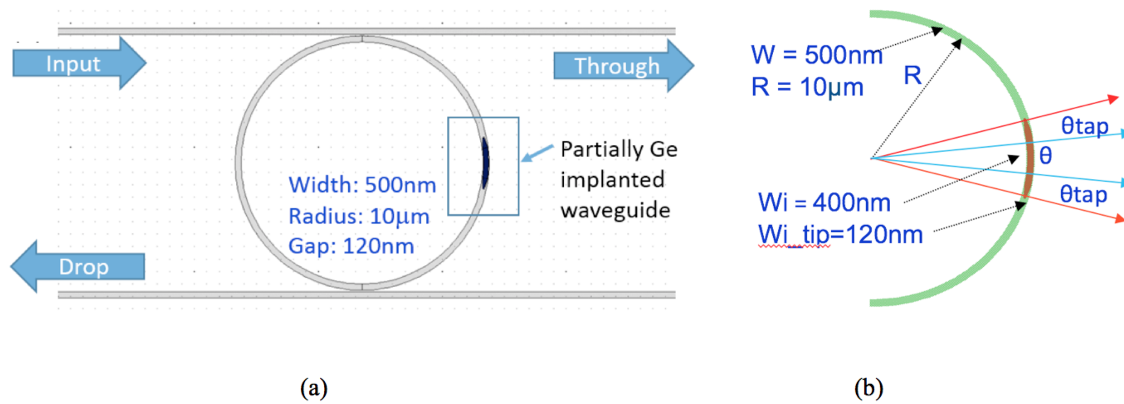

Figure 1. a) A schematic of ring resonators with a section of amorphous silicon created by Ge ion implantation. The waveguide is 500 nm wide, while the ring radius is equal to 10µm. (b) A detailed layout of Ge ion implanted waveguide section. The ion implanted region is 400nm wide and is located in the center of the ring waveguide. A short ion implanted taper, with a tip width of 120 nm, was attached to both ends of ion implanted waveguide section.

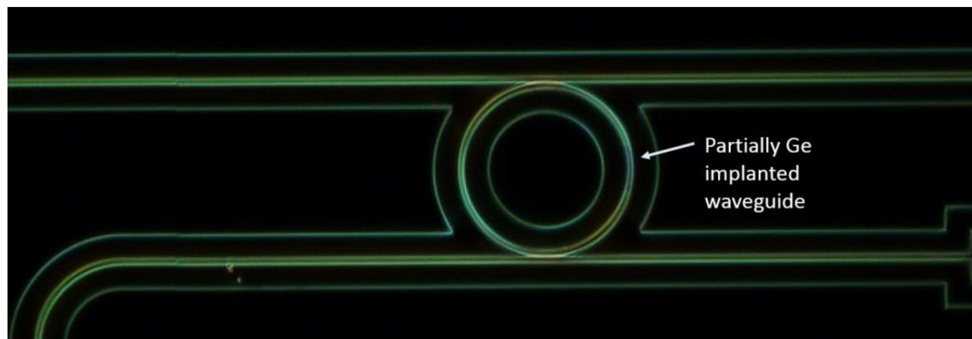

Figure 2. An optical microscope image of the ring resonator with a partially ion implanted Ge waveguide section.

The layout of the Ge implanted section is shown in Figure 1b. The arc length of the ion implanted section is denoted by angle θ. The width of ion implanted region, located in the center of silicon rib waveguide, was equal to 400 nm. A short taper, with a tip width of 120 nm, was formed at both ends of the ion implanted region (θtap=5°), in order to reduce reflection of light between the silicon and Ge ion implanted regions of the waveguide, and potential resonance inside the ion implanted waveguide section. Rib waveguides and ring resonators were fabricated by electron beam lithography. A 20 nm thick PECVD oxide was deposited as a protective layer. After this fabrication step, a photoresist layer was

deposited as a mask layer for Ge ion implantation. An ion energy and fluence of 130KeV and $1x10^{15}$ ions/cm^2 were used, respectively. According to our previously results[1,2], this will provide 80% lattice disorder in silicon with a refractive index change of 0.5. An optical microscope image of a fabricated ring resonator is shown in Figure 2. Simulation results are presented in Figure 3a. As it can be seen, an ion implanted ring resonator ($\theta = 22^o$) is predicted to experience a red shift of the resonant wavelength peak.

We have explored the same ion implantation technique to investigate the coupling efficiency of Ge ion implanted grating couplers for various numbers of grating widths in the 220nm SOI platform. Design and fabrication were performed following the same steps as for ion implanted ring resonators. Simulations were performed using Lumerical software[9] (Mode solutions). If not stated otherwise, all results are obtained for the fundamental TE mode at an operating temperature of 20 °C at 1550 nm wavelength, and a germanium ion implantation depth of 130 nm. Figure 3b shows 2D simulation results for grating coupler efficiency as a function of grating width assuming a large enough number of grating lines (~30). As can be seen, low insertion losses may be achieved for grating widths larger than 10 µm.

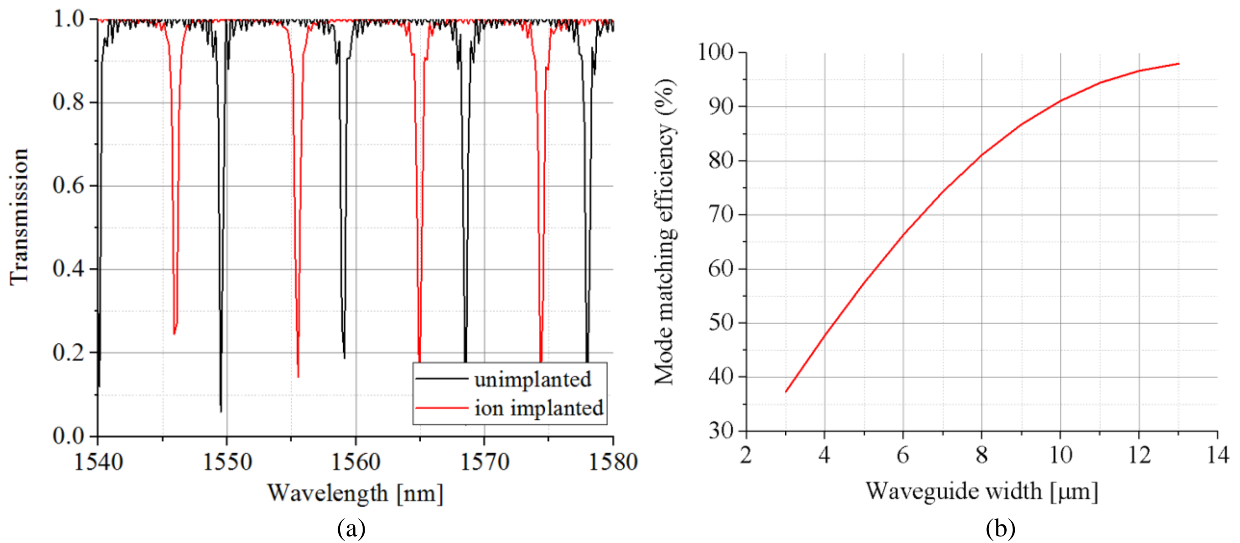

Figure 3. Simulation results of implanted devices. (a) Transmission spectrum of an un-implanted and Ge ion implanted ring resonator. (b) Lateral grating coupler mode matching efficiency as a function of grating width.

3. EXPERIMENTAL RESULTS

A tunable laser with a wavelength range from 1520 to 1620 nm was used to characterize the fabricated devices. To accurately measure the output signal, we used a sample stage with a Peltier element to keep the temperature constant during measurements (20°C). Shallow etched (70nm) gratings optimized for TE polarization were used at the input/output of the waveguide to provide efficient coupling of light from/to the single-mode optical fibers used for testing. The results presented in this paper are for wavelengths around λ~1550 nm. However, similar results have been obtained at other wavelengths.

Figure 4 shows a typical transmission spectrum comparing the performance of an un-implanted ring resonator and Ge ion implanted ring resonators with various implantation lengths. The resonant wavelength peak of an un-implanted ring resonator revealed resonant wavelengths at 1560.5 nm and 1570.4 nm. A clear trend of the resonant wavelength shift was observed for implanted resonators. The resonant wavelength shifted to longer wavelengths as implantation length increased due to higher mode interaction with the amorphous silicon. It can be seen that a resonator with an implantation arc length of $\theta=22°$ does not conform to this trend. This may be caused by a sudden change in electron beam position or unwanted contamination during device fabrication, but has yet to be explained. Measured ring resonators exhibited an

extinction ratio of over 24 dB and a similar spectrum shape. It is worth mentioning that the measured devices were very close to each other on the same chip thus keeping the SOI wafer thickness variations and fabrication difference between each device to a minimum. The results also showed that ion implanted waveguide sections only induced a very small amount of loss, which didn't degrade the overall performance of ring resonators significantly.

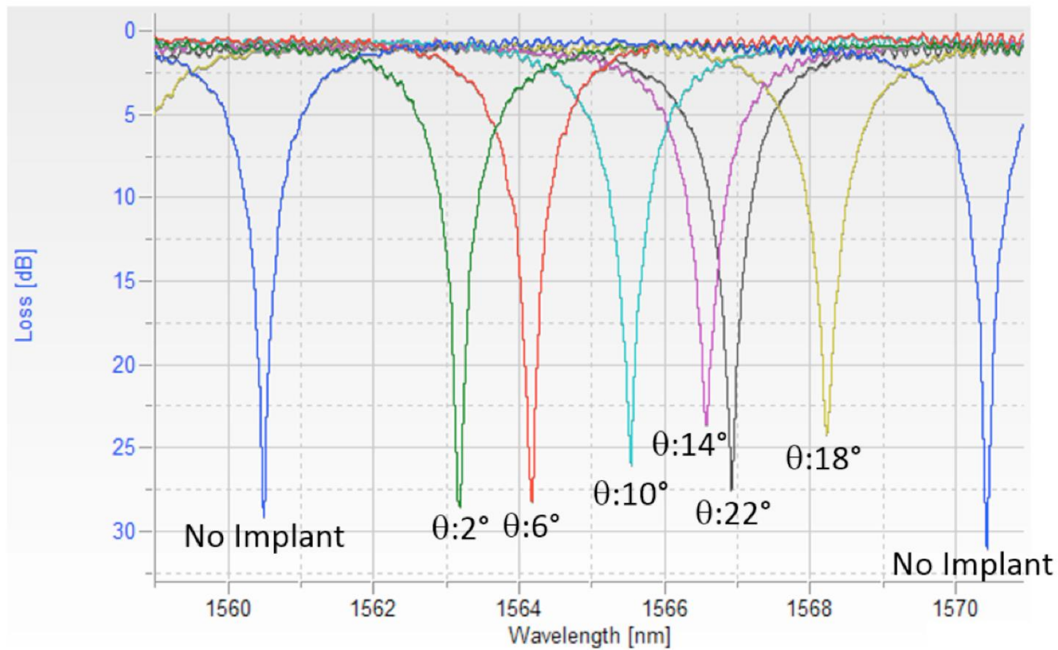

Figure 4. Transmission spectra of fabricated ring resonators with various implantation lengths. As implantation length increases, resonant wavelength peak shifts to longer wavelengths.

The refractive index of implanted silicon is about 3.96, which could be gradually reduced to 3.47 by cycles of rapid thermal annealing (RTA). It can be additionally controlled by adjusting the annealing time, thus shifting the resonant wavelength to a target position. Therefore, a one minute RTA was carried out to partially anneal the implanted silicon regions at different temperatures. It was found that an annealing temperature of 250°C caused essentially no change in the position of the resonant wavelength. However, at higher temperatures a clear blue shift was observed. Figure 5 shows the comparison of the transmission spectrum between an un-implanted ring resonator and the implanted ring resonator ($\theta=18^{\circ}$) at different annealing temperatures of 350 ºC and 450 ºC, respectively. The FWHM of those spectra are 1.76 nm (Ref), 1.53 nm (350°C) and 1.46 nm (450°C), which corresponded to a Q-factor of 891, 1024 and 1071. It can be seen that Q factor increased as annealing temperature was increased, showing that the reduction of the round-trip loss of the ring cavity by applying the thermal annealing technique.

Figure 6 shows the resonant wavelength shift for various implantation lengths and annealing temperatures of 350°C, 450°C and 500°C. The effective length of the ion implanted waveguide region was calculated to include ion implanted tapers on both ends of the ion implanted region of the waveguide. A very linear relationship between the resonant wavelength shift and implantation length was observed. The shift was very low at small annealing temperatures and it increased at higher temperatures due to change in refractive index of the implanted region. It can be seen that an implantation length of 6 μm would provide a resonant wavelength shift of 10 nm, which corresponds to the free spectral range of fabricated ring resonator. For practical applications, the trimming of individual rings can also be done by localized laser annealing[1,2].

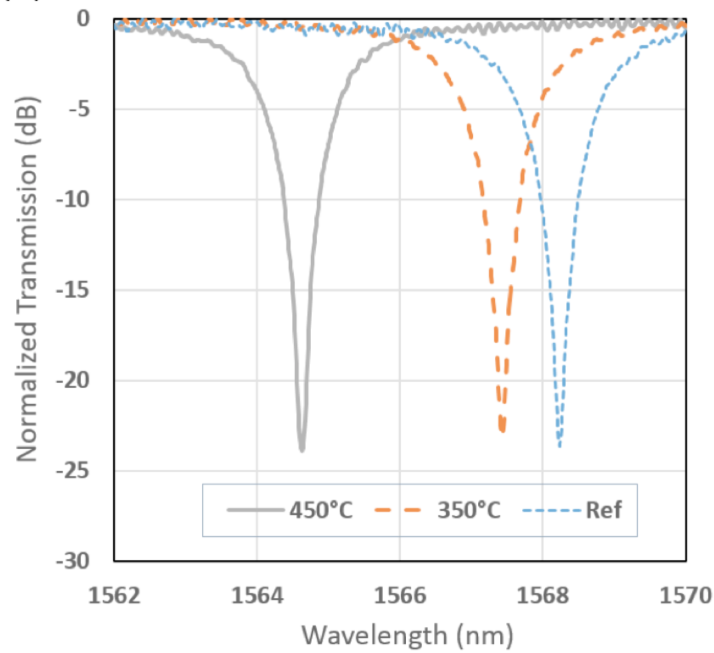

Figure 5. Transmission spectrum of Ge ion implanted ring resonator with θ=18° before annealing (ref), and corresponding transmission spectrum after 350°C and 450°C RTA for 1 min.

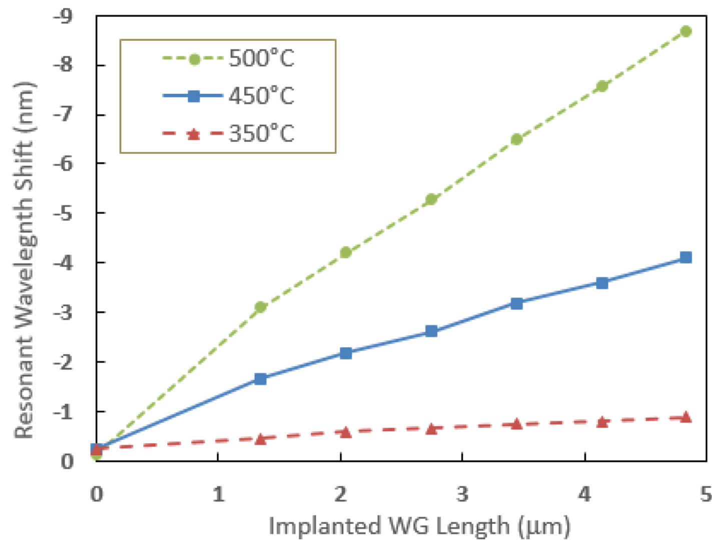

Figure 6. Resonant wavelength shift as a function of implantation length at different annealing temperatures.

Trimming stability experiments were also performed. The samples were left in the oven at 220 ºC for one day and then a further week. The resonator wavelength shift followed the same trend as before, the wavelength shift increased for

longer implantation lengths, however the maximum overall shift was always between 0.07 nm and 0.3 nm during a period of 8 days. Further testing on the stability and reliability of this technique are ongoing.

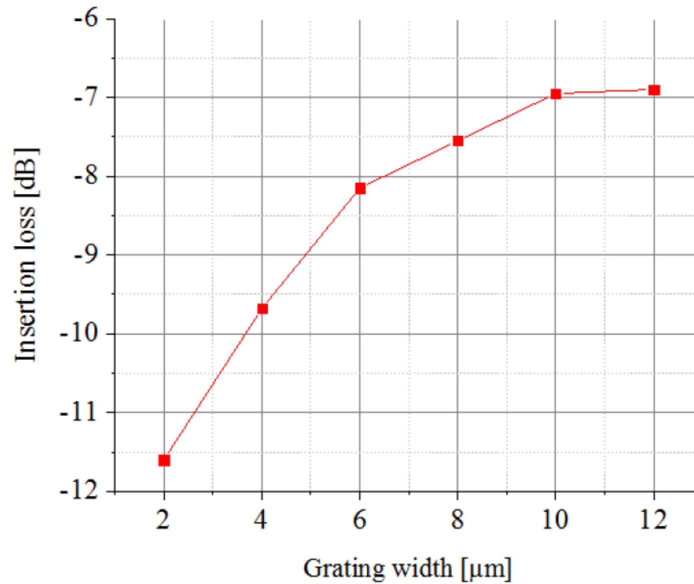

Figure 7. Insertion loss of germanium ion implanted grating coupler at different grating widths.

Figure 7 shows experimental results for ion implanted grating couplers as a function of grating width. As expected, lower loss was achieved for wider gratings, ranging between 6.9 dB and 11.5 dB per grating for grating widths between 12 and 2 µm, respectively. Ion implantation process brings with it the ease of device fabrication, including precise and repeatable grating depth control which is more difficult to obtain with a standard etching process. Therefore, an accurate design of the grating and optimisation of the fabrication process are expected to be crucial for large scale manufacturing and wafer scale testing of photonic integrated circuits.

CONCLUSIONS

We performed simulation and experimental analysis on trimming the position of the resonant wavelength peak of silicon ring resonators and investigated coupling efficiency of ion implanted grating couplers using Ge implantation technique. Partial annealing of the ion implanted section revealed the possibility to permanently adjust the resonant wavelength peak position to a target wavelength. Grating coupler efficiency increased for wider grating widths, however, a longer taper will be required to use this device for wafer scale testing purposes. The process is CMOS compatible and can be transferable to other platforms and systems such as multilayer photonics and programmable photonic circuits.

ACKNOWLEDGEMENTS

This work was funded by EPSRC project under the “Silicon Photonics for Future Systems” “Electronic-Photonic convergence” and “CORNERSTONE” projects. Reed is a Royal Society Wolfson Research Merit Award holder. He is grateful to the Wolfson Foundation and the Royal Society for funding of the award. . CGL and HW acknowledge support from National Research Foundation of Singapore (NRF-CRP12-2013-04).

REFERENCES

[1] Topley R., O'Faolain L., Thomson D. J., Gardes F. Y., Mashanovich G. Z., and Reed G. T., "Planar surface implanted diffractive grating couplers in SOI," Optics Express 22, 1077-1084 (2014).

[2] Topley R., Martinez-Jimenez G., O'Faolain L., Healy N., Mailis S., Thomson D. J., Gardes F. Y., Peacock A. C., Payne D. N. R., Mashanovich G. Z., and Reed G. T., "Locally erasable couplers for optical device testing in silicon on insulator" Journal of Lightwave Technology 32(12), 2248-2253 (2014).

[3] Milosevic M. M., Emerson N. G., Gardes, F. Y., Chen X., Adikaari A. A. D. T., Mashanovich G. Z., "Athermal waveguides for optical communication wavelengths," Optics Letters, 36(23), 4659-4651 (2011).

[4] Reed G. T., Mashanovich G., Gardes F. Y., Thomson D. J., "Silicon optical modulators," Nature Photonics 4, 518-526 (2010).

[5] Bogaerts, W., De Heyn P., Van Vaerenbergh T., De Vos K., Selvaraja S. K., Claes T., Dumon P., Bienstman P., Van Thourhout D., and Baets R., "Silicon microring resonators," Laser Photonics Review 6**,** 47-73 (2012).

[6] Schrauwen J., Van Thourhout D., and Baets R., "Trimming of silicon ring resonator by electron beam induced compaction and strain," Optics Express 16, 3738-3743 (2008).

[7] Prorok S., Petrov A. Y., Eich M., Luo J., and Jen A. K.-Y., "Trimming of high-Q-factor silicon ring resonators by electron beam bleaching," Optics Letters 37, 3114-3116 (2012).

[8] Heidemann K. F., "Complex-refractive-index profiles of 4 MeV Ge ion-irradiation damage in silicon," Philosophical Magazine B 44(4), 465-485 (1981).

[9] www.lumerical.com